

Development & Application of modern Measurement Techniques for pressurised cryogenic Wind Tunnels

J. Quest, J. Leuckert*, U. Fey, R. Konrath**, Y. Egami****
ETW GmbH, *TU-Berlin, **DLR

Keywords: *Wind tunnel testing, cryogenic, instrumentation, PSP, PIV, PSC*

Abstract

The present paper addresses the development, qualification trials and application of some modern measurement techniques suitable for operation in the pressurised cryogenic wind tunnel ETW. Enhanced online model deformation measurement systems as well as techniques for boundary layer analysis like hot-films, hot-wire arrays and copolymers are described and the progress on the development of cryo-PSP and cryo-TSP is reported. The considerations for an establishment of cryo-PIV are presented.

1. Introduction

Flight Reynolds number testing on scaled aircraft models is presently only performed in the European Transonic Windtunnel ETW in Germany and the National Transonic Facility NTF in the US. Both facilities are applying the same concept regarding the generation of the relevant test conditions by using moderately compressed pure nitrogen at cryogenic temperatures as test gas. During the recent decade achieved benefits of this simulation technique could impressively be demonstrated leading to modifications of modern aircraft design chains revealing a fruitful cooperative application of numerical design tools and wind tunnel testing. As an outcome of this symbiosis customers expressed additional needs for information about the flow field around the model as well as its behaviour in addition to the classical force, pressure and moment measurements. The status and progress of relevant techniques is addressed in this paper.

2. Facility description (ETW, PETW)

The ETW facility is a wind tunnel of Eifel type featuring slotted or solid walls. The Mach number ranges from 0.15 to 1.35 while the Reynolds number can be established by combinations of pressure (115 to 450 kPa) and temperature (115 to 313 K), hence, allowing pure Reynolds number or pure aeroelastic investigations. The test section dimensions are 2.4 x 2 x 9m (width x height x length).

For cost saving research and development activities are typically performed in the pilot facility PETW, which is a geometrically correct scaled down version by a factor 8.8 regarding its high speed leg. Manual access is provided after the removal of the front flange and opening of the test section sidewall (door) equipped with a window for optical access or a remotely controlled drive for incidence variations of 2d-models horizontally spanning the test section. A global view of PETW is given in Fig. 1.



Fig 1: The cryogenic Pilot facility PETW

3. Surface measurements

Ideally, all applied techniques should be non intrusive especially regarding the thin boundary layers on surfaces at high Reynolds numbers. Several investigations have proven a surface finish of $Ra \leq 0.2 \mu\text{m}$ to be adequate when considering a fully turbulent flow but better finish is to be required for natural laminar flow simulations.

3.1 Techniques based on coatings

Relevant applications are based on single or multi-layer spraying on the metallic surfaces with subsequent polishing, if feasible.

3.1.1 Pressure Sensitive Paint (cryo-PSP)

The conventional way of acquiring surface pressures on a model is by pressure-plotted models. This method is well-known and widely used but contains drawbacks: the pressure measurement is performed at discrete locations, the installation of pressure ports in a wing is a long and costly action, it limits the maximum wing load capacity and can therefore reduce the test envelope. Consequently, Pressure Sensitive Paint (PSP), which can overcome these drawbacks, is of great interest. However, the application of PSP in cryogenic wind tunnels is not straightforward because the test conditions in a cryogenic wind tunnel are quite different from those of conventional wind tunnels as shown in **Table 1**.

	Oxygen concentration	Temperature
Cryogenic wind tunnel	< 0.2% (2000ppm)	110 – 180K
Conventional wind tunnel	21%	~300K

Table 1: Different test condition between cryogenic- and conventional-wind tunnels

Cryogenic wind tunnels use evaporated liquid nitrogen as a test gas to decrease the tunnel temperature down to 100 K (-173°C).

Hence, oxygen needs to be added artificially but is limited to several thousands of ppm for safety reasons. In addition, the low

oxygen of a polymer binder resulting in a low pressure sensitivity of PSPs. Consequently, most conventional PSPs are not suitable for cryogenic test conditions requiring developing a cryo-PSP with oxygen sensitivity high enough to measure a small change of oxygen-partial pressure even at cryogenic test conditions. First trials have been made in the PETW in August 2004, followed by a test in ETW in October. In both tunnels an oxygen injection, homogenous distribution and measurement of its concentration with the desired accuracy could be achieved. At least, in both facilities an oxygen concentration between 500 and 2000 ppm could be established and kept constant to $\pm 5\text{ppm}$ during the acquisition of PSP images, which is supposed to be sufficient for PSP measurement at cryogenic conditions. A cryo-PSP developed by DLR was applied to a research full model released by AIRBUS-UK by using an airbrush as shown in **Fig. 2**. An evaluation test was carried out at the ETW.

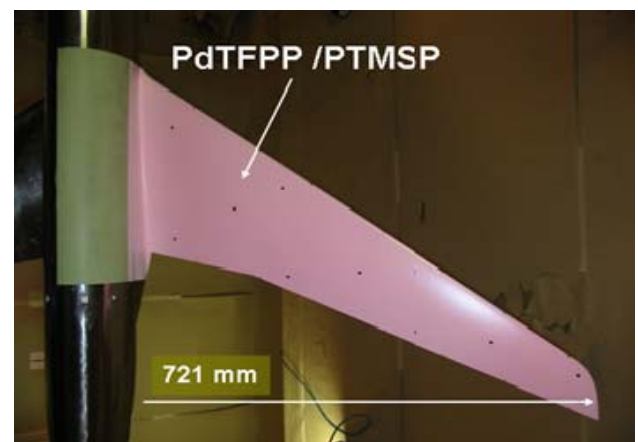


Fig 2: Research full model used for the first PSP test in ETW

Fig.3 shows pressure fields on the PSP covered wing obtained at (a) $T=260\text{ K}$ and (b) $T=160\text{ K}$ at $Ma=0.85$.

Black regions in the figures represent low pressures and grey areas high pressures. In this very first PSP test in ETW the surface pressure distribution shows some interesting details, not resolvable with pressure taps. In **Fig.3(a)**, the pressure step due to a shock wave is visualised. In addition, we can observe longitudinal vortex structures near the wing tip. In **Fig.3(b)**, two separated low pressure regions are observed.

The obtained absolute pressure distribution at 40% of the wing span of Fig.3(b) is plotted in Fig.4 in comparison to PSI data. The calculated PSP pressure along the line cut shown in Fig.4(b) using in-situ calibration, gives a qualitative agreement. So these first trials looked promising, and further PSP development has been performed by DLR to increase the sensitivity and accuracy of the paint.

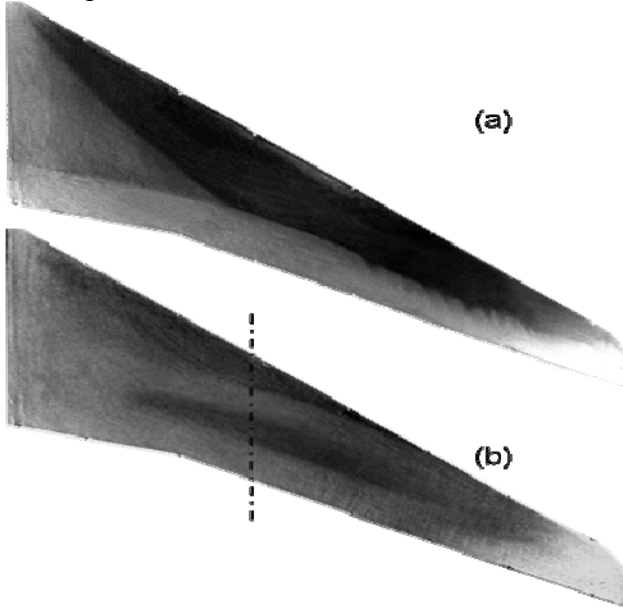


Fig.3: Results of evaluation test at ETW at $\chi=0.007$ (700 ppm): (a) $T=260$ K, $Ma = 0.85$, $Re=4.8$ M, $p=125$ kPa, $\alpha_0=0.30$ deg. and (b) $T=160$ K, $Ma = 0.85$, $Re=25$ M, $p=340$ Pa, $\alpha_0=0.09$ deg.

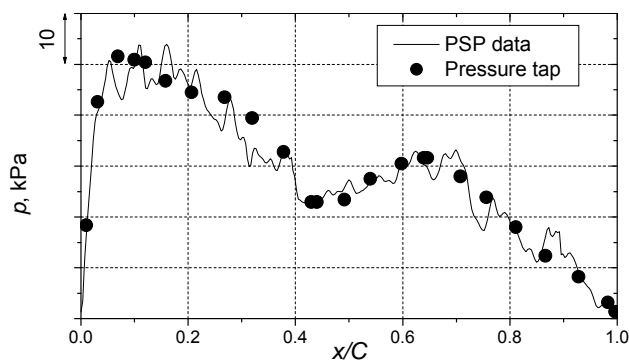


Fig.4: Pressure distribution of Fig. 3(b) at 40% span (dashed line).

3.1.2 Temperature Sensitive Paint (cryoTSP)

With respect to future aircraft design, Natural Laminar Flow (NLF) and Hybrid Laminar Flow Control (HLFC) are favoured techniques with a potential for further reduction of aerodynamic drag. Optimization of NLF and

HLFC in ETW and improvement of the computational prediction methods require experimental techniques to determine a wind tunnel model's boundary layer state under cryogenic conditions. As the application of the IR technique is limited to temperatures above 200K an alternative has been found in cryo-TSP which is based on the *thermal quenching* mechanism of molecules embedded in the paint. Luminophores are excited by incident light of a certain wavelength (for example UV or blue light) which sends the molecules to an excited state. Subsequently the excited molecules drop back to the ground state by emission of light of a longer wavelength (for example red). Additionally, there exists a process of deactivation without light emission whose rate is dependent on the heat content of the paint. The higher the temperature of cryo-TSP, the more molecules drop back without light emission and the paint appears darker in comparison to colder regions.

Generating a temperature step in the main flow warmer or cooler with respect to the model it will be transferred faster to the coated surface across the turbulent boundary layer. This is because of the different heat transfer coefficients in the turbulent and laminar boundary layers. Hence, the transition line occurs as a borderline between dark and light areas of a TSP image taken during the step change (see Fig.5).

Artificial heating may enhanced this process[1].

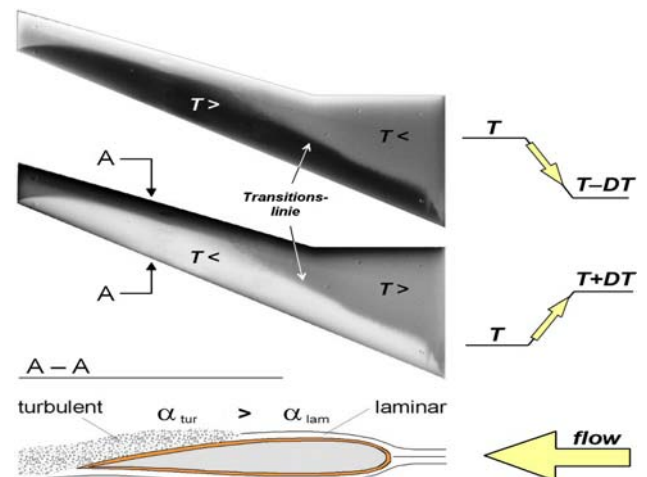


Fig 5: Visualization of laminar-to-turbulent boundary layer transition by means of cryo-TSP, using temperature changes of $+DT$ or $-DT$ superimposed to the oncoming flow.

Transition detection using cryo-TSP has been successfully applied in ETW together with the DLR Institute of Aerodynamics and Flow Technology since the beginning of 2003, initially in strong cooperation with the Japanese Aerospace Exploration Agency (JAXA, formerly NAL[2]). The original cryo-TSP paint has been developed by JAXA optimised for application in large, industry-scale wind tunnels[3].

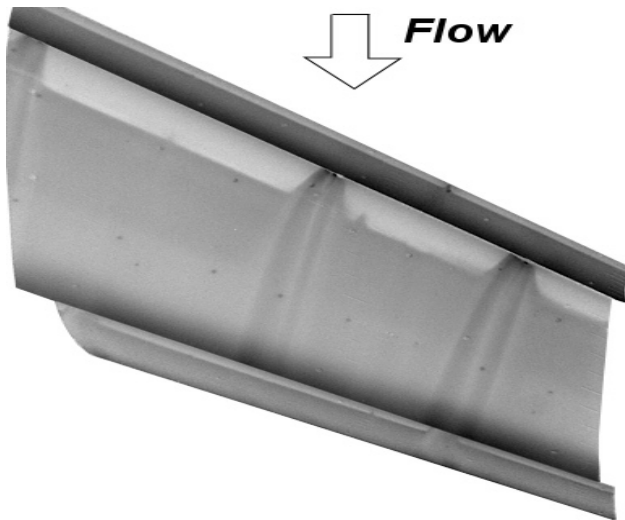


Fig 6: Application of 2C-cryoTSP on a half model wing in landing configuration. Transition is shown on the slat, the main wing and the flap. Bright gray areas: laminar-parts, dark gray areas: turbulent parts of the boundary layers. $T = 290\text{ K}$, $M = 0.24$, $Re = 9\text{ Mio}$

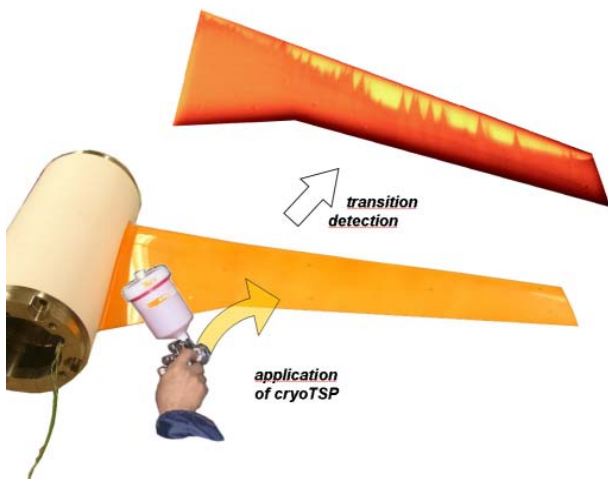


Fig.7: Application of cryo-TSP to a wind tunnel model's wing by use of a spray gun. The paint can be polished to high smoothness as recommended for cryogenic testing. The luminophor Ruthenium complex $\text{Ru}(\text{trpy})$ is embedded in a transparent Polyurethan binder and the paint can easily be sprayed on the model surface using a spray gun (Fig.7). Within the last years, the DLR Institute of

Aerodynamics and Flow Technology has continuously improved the cryo-TSP technique in co-operation with ETW and new paints have been designed to extend the application range of the temperature-sensitive paint method. For example, a two-component cryogenic TSP (2C-cryo-TSP) was developed allowing to cover the complete temperature range of ETW from 300 K down to 100K using a single coating with different excitation light only[4].

3.1.3 Liquid-crystals (LC)

For wind tunnels operating at environmental temperatures surface coatings with oil, oil based mixtures or acenaphthene represent standard and mature methods for the visualisation of flow separation. By nature, those ingredients are not suitable for cryogenic environment with their additional drawback to require a re-coating for each individual test condition. Searching for alternatives led to the consideration of liquid crystals featuring nano dimensions and being sprayable using a suitable solvent [5]. First basic experiments performed in ETW and PETW [6] confirmed the general qualification of those crystals and allowed a ranking and selection of the different types available. A typical test result showing the capabilities of crystals for flow analysis is given by Fig. 8. With respect to the primary objective to indicate flow separation the shear sensitive crystal type known as “Chiral nematics” revealed the most promising type also due to their fast response. They consist of staggered layers of molecular structures forming a helix, which will be disturbed by the application of shear stress. Finally, the pitch of the helix (proportional to the wavelength of the reflected light) will cause a colour change related to the level of shear stress applied.

So, new liquid crystals with adapted dopants to manage the wavelength of the reflected light suitable to be operated at cryogenic temperatures have been developed. Presently, the test set-ups for validation tests in PETW are under preparation.

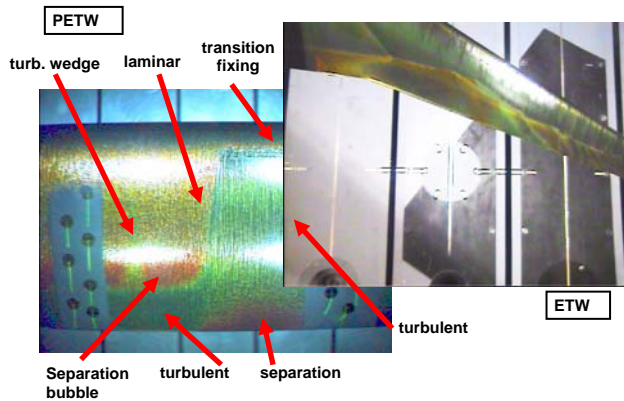


Fig 8: Flow visualisation by liquid crystals

3.2 Temporal and Spatial Resolvable Surface Measurement Techniques

Especially for the detection of characteristic frequencies of flow instabilities, a high temporal resolution is needed. Since both, the newly developed Pressure Sensitive Copolymer technique and the surface hot-wires, provide a high spatial and temporal resolution, these methods were applied to wind tunnel models for transition experiments. In order to characterise transition, the signals were analysed using different statistical quantities. The Root Mean Square (RMS) values were calculated to obtain information about the mean fluctuation amplitude. Increased RMS values indicate regions with high levels of local fluctuations, e.g. a transitional boundary layer [7]. Additionally, power spectra were calculated to determine characteristic frequencies.

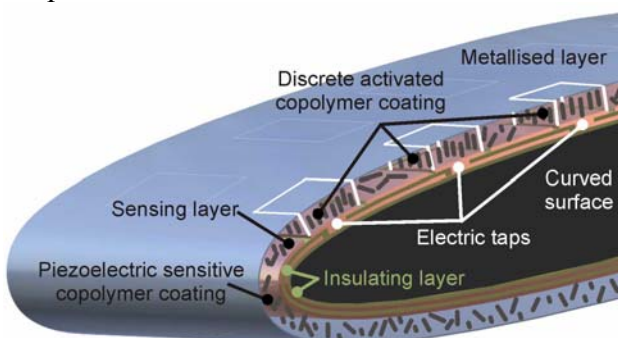


Fig.9: Principle of Pressure Sensitive Copolymer Coating

3.2.1. Transition Detection on a 2D Airfoil Model by Applying Pressure Sensitive Copolymer Coating

Within the framework of the EC Project „Fliret“, the influence of leading edge

roughness on the laminar turbulent transition was investigated on a 2D model. This model was equipped with a Pressure Sensitive Copolymer (PSC) coating in addition to Temperature Sensitive Paint applied by the DLR (German Aerospace Center) and pressure taps measuring the mean pressure distribution. The experiments have been carried out in the PETW.

3.2.1.1. Principle of Pressure Sensitive Copolymer Coating (PSC)

$$E(Q) = d_{33} p' A_{sensing} \quad (1)$$

Generally, the Pressure Sensitive Copolymer coating relies on the piezoelectric properties of the copolymer of vinylidene fluoride and trifluoroethylene. Thus, PSC reacts with an electrical polarisation (Q) caused by an unsteady pressure (p') on a discrete sensing area (A_{sensing}). The electrical polarisation is converted into measurable voltage (E) by electronic charge amplifiers. This linear relationship is expressed in Eq. (1), where d₃₃ is the piezoelectric constant of a normal charge displacement parallel to the pressure fluctuation, which depends on the piezoelectric material. The principle of Pressure Sensitive Copolymer coating is presented in Fig. 9. The PSC is sprayed onto a sensing layer of an electroconductive carrier material. Typically, a copper coated capton foil or circuit board is used. Thereby, various sensing and electrical layouts can be produced by photo etching and adapted to arbitrary applications. Furthermore, surface roughness from the electrical connections is minimised by the separation of the sensing elements from the electrical taps. After spraying the piezoelectric copolymer onto the sensing layer, it is not yet sensitive, because the crystallites of the copolymer are not orientated. Consequently, the sensing elements of the PSC coating are discretely activated by a corona discharge, whereby a variable matrix of sensitive elements is achieved. Finally, the surface is vacuum metallised with a very thin layer of copper.

3.2.1.2. Experimental Set-up

The Pressure Sensitive Copolymer coating was based on a special multilayer circuit board, which was inserted flush mounted into a cut-out machined into the surface of the model. The instrumented PETW model with a chord length of 100mm is presented in Fig.10

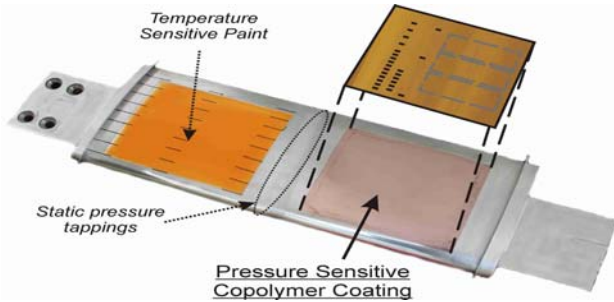


Fig.10: Instrumented 2D airfoil model for transition experiments on the influence of leading edge roughness performed in the PETW

The PSC sensing layer consisted of 24 active elements. The elements with a size of 1.5mm (stream wise) \times 3mm (span wise) were staggered in three rows covering a range $0.20 \leq x/c \leq 0.74$. The PSC signal path was shortened by designing the final layer with integrated electronic charge amplifiers. The necessary electronic components were soldered directly onto the final layer of the PSC circuit board and stored into three deeper cavities, which were additionally machined into the PSC pocket. The PSC coated and electronically equipped circuit board was applied flush mounted into the model by a vacuum gluing method. Thereby, additional surface roughness was minimised and curvature modification prevented. Finally, the Pressure Sensitive Copolymer coating was vacuum metallised with a 200nm copper layer.

3.2.1.2. Experimental Results

The experiments were performed at a constant free stream Mach number of $M_\infty = 0.24$ with different angles of attack and Reynolds numbers in the range of $1.0 \cdot 10^6 \leq Re \leq 4.0 \cdot 10^6$. The dependence of transition on these Reynolds numbers was investigated for a fixed angle of attack of $\alpha = 1.0^\circ$ and a leading edge roughness of $R_z = 7\mu\text{m}$. The leading edge was

roughened in the area between 5% chord of the pressure side and 2% chord of the suction side.

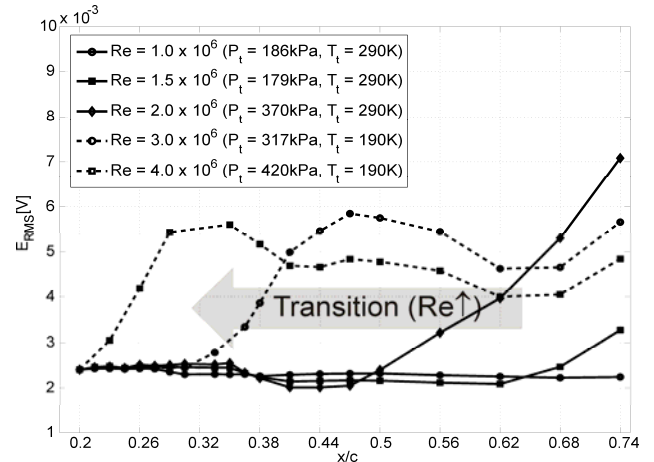


Fig.11: RMS distributions of PSC obtained at leading edge roughness of $R_z = 7\mu\text{m}$, $M_\infty = 0.24$, $\alpha_\infty = 1.0^\circ$ and various Reynolds numbers

The obtained RMS distributions are shown in Fig 11. The constant low RMS level for $Re = 1.0 \cdot 10^6$ ($P_t = 186\text{kPa}$, $T_t = 290\text{K}$) all over the sensing area clearly indicates the laminar boundary layer. The transitional boundary layer along with increased pressure fluctuations is detected by the step-up of the RMS values at $x/c > 0.62$ and $x/c > 0.50$, when the Reynolds number is increased to $1.5 \cdot 10^6$ ($P_t = 179\text{kPa}$, $T_t = 290\text{K}$) and $2.0 \cdot 10^6$ ($P_t = 370\text{kPa}$, $T_t = 290\text{K}$). A further increase of the Reynolds number leads to an upstream shift of the rise of the RMS values, thus indicating the upstream shift of the laminar turbulent transition. The turbulent boundary layer downstream of $x/c \geq 0.41$ for $Re = 3.0 \cdot 10^6$ ($P_t = 317\text{kPa}$, $T_t = 190\text{K}$) and $x/c \geq 0.62$ for $Re = 4.0 \cdot 10^6$ ($P_t = 420\text{kPa}$, $T_t = 190\text{K}$) is detected by the nearly constant but significantly higher RMS level compared with the laminar flow.

3.2.2 Hot-film arrays for boundary layer analysis

Transition detection by temperature sensitive paint has been evaluated as a mature technique for wings and flaps. Regarding the leading edge area of e.g. slats of high lift configurations the restricted optical access in wind tunnels requires the application of other techniques. While hot-films were thought to suffer signal problems at lower temperatures due to heat

exchange with the model itself surface hot-wire arrays may be inaccurate due to generated disturbances of the near wall flow caused by the wire. So, it had been decided to perform comparative validation tests in PETW down to cryogenic temperatures. A swept wing model as shown in Fig.12 was prepared and instrumented with both techniques.



Fig. 12 Swept airfoil model equipped with surface hot film array (DLR, left) and surface hot wire array (TU Berlin, right)

Covering the full operating envelope of PETW both systems successfully demonstrated their capabilities leading to the instrumentation of the inboard slat of a half-model for subsequent

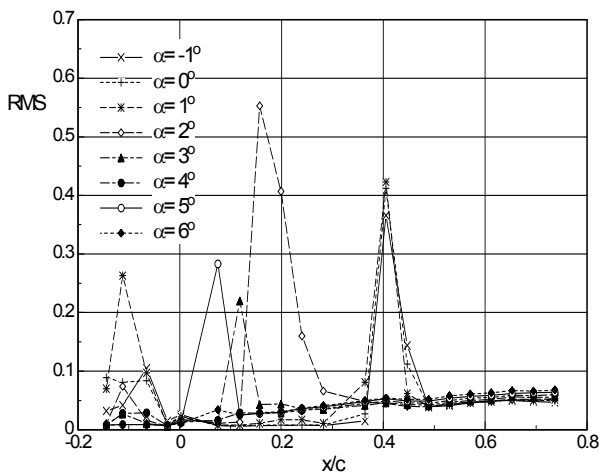


Fig. 13: RMS distributions, MR 8, Ma=0.2, p_t= 2.9 bar, T_i= 120 K, Re= 3.0×10⁶

testing in ETW. Fig. 13 presents the assessed forward shift of the boundary layer transition as function of the angle of attack at severe cryogenic conditions. The Reynolds number is based on model chord.

From the ETW entry it can be concluded that both techniques are generally qualified for the defined objective but the drawback of running

a pair of small wires for each sensors has to be kept in mind for both.

3.2.3. Transition Detection on a 2D Swept Airfoil Model by Applying a Surface Hot-Wire Array

The performance of the surface hot-wire measurement technique under cryogenic conditions was investigated within the framework of the EC Project „Eurolift II“. The transition experiments have been carried out on a 2D swept airfoil model in PETW (see Fig. 12). Additionally, the model was equipped with a surface hot-film array designed by DLR.

3.2.3.1. Principle of a Surface Hot-Wire

The surface hot-wire measurement technique is based on the forced convection of a heated wire analogous to the conventional hot-wire anemometry. In Fig 14 the principles of a single surface hot-wire is shown. In contrast to a conventional hot-wire, which is soldered on a probe, a surface hot-wire is welded over a narrow cavity on an electro conductive carrier material [8].

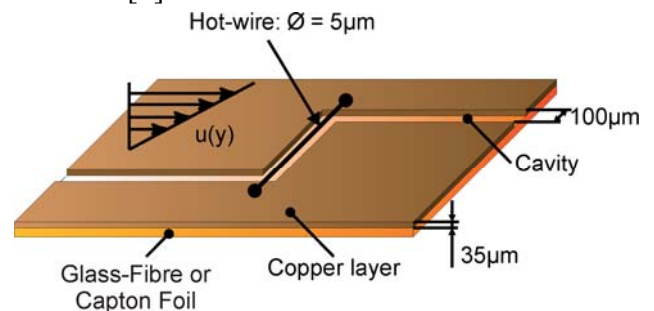


Fig. 14: Principle of a single surface hot-wire sensor

Arbitrary and tightly packed sensor layouts can be produced by a photo etching process into a copper coated capton foil or glass fibre circuit board, depending on the application.

A platinum-coated tungsten wire with a diameter of 5µm is used as the sensor. Principally, surface hot-wires are sensitive to the flow velocity just like conventional hot-wires. However, considering the small wire diameter and thus, the small constant wall distance, a correlation between the flow velocity and the local wall shear stress exists. The sensors are operated in the constant temperature mode using Wheatstone bridges.

The bridge output voltage level is proportional to the local wall shear stress amplitudes.

3.2.3.2. Experimental Set-up

The surface hot-wire array was based on a copper coated capton foil consisting of stream wise as well as span wise oriented sensors. The sensor array covering an area of $0.10 \leq x/c \leq 0.21$ was applied from the suction side around the leading edge to the pressure side. To minimise additional roughness, the surface hot-wire array was inserted into a cat-out machined into the surface of the model utilising a vacuum gluing method. In Fig. 12 the instrumented model with a chord length of 68mm and a leading edge sweep. The sensors were connected on the pressure side to very thin insulated cooper wires with a diameter of 0.2mm. These wires were laid into a cut inside the wing to minimise the influence on the flow field. The insulated wires were connected to co-axial cables for the data link to the multi-channel constant temperature anemometer outside of the test section. For the simulation of ETW test conditions, special micro-coax cables were used. These cables had a length of 25m and a very low specific cable resistance. Therefore, the cable resistances were significantly lower than the sensor resistances. Furthermore, two-thirds of the cable length was laid into the plenum of the wind tunnel to correctly simulate the ETW conditions along the cables.

3.2.3.2. Experimental Results

The experiments were performed at a constant free stream Mach number of $M_\infty = 0.2$ with various angle of attack and Reynolds numbers in the range of $0.42 \cdot 10^6 \leq Re \leq 4.25 \cdot 10^6$. The dependence of the characteristic instability frequency range on these Reynolds numbers was determined for a fixed angle of attack $\alpha_\infty = 3.0^\circ$. The spectra for a selected surface hot-wire sensor at the stream wise position of $x/c = 0.10$ presented in Fig 15, demonstrate the step-up of the centre frequency with increasing Reynolds number. For a Reynolds number of $Re = 0.42 \cdot 10^6$ ($P_t = 120\text{kPa}$, $T_t = 290\text{K}$), the

centre frequency of $F = 8.4\text{kHz}$ can clearly be identified.

When the Reynolds number increases to $Re = 1.11 \cdot 10^6$ ($P_t = 326\text{kPa}$, $T_t = 290\text{K}$), the centre frequency is obviously shifted to $F = 11.2\text{kHz}$. Furthermore, the influence of total pressure and temperature is determined. Therefore, two curves representing the same Reynolds number ($Re = 1.11 \cdot 10^6$) at different temperature and pressure are shown in comparison. Due to the individual adjustment of the surface hot-wire sensors for each flow temperature, there is a slight difference in the general level of the magnitude. Additionally, the increase of the magnitude at $F = 7.5\text{kHz}$ for the low temperature is probably caused by the electronics due to the insufficient adjustment of the sensor. However, the characteristic frequency range can be concordantly determined for both flow conditions. Moreover, the magnitude level is significantly increased all over the frequency range and thus indicates the later stage of the transition compared to $Re = 0.42 \cdot 10^6$.

An additional rise in the Reynolds number leads to a further shift of the centre frequency to $F = 12.6\text{kHz}$ for $Re = 3.15 \cdot 10^6$ ($P_t = 290\text{kPa}$, $T_t = 125\text{K}$) and $F = 13.8\text{kHz}$ for $Re = 4.25 \cdot 10^6$ ($P_t = 387\text{kPa}$, $T_t = 125\text{K}$).

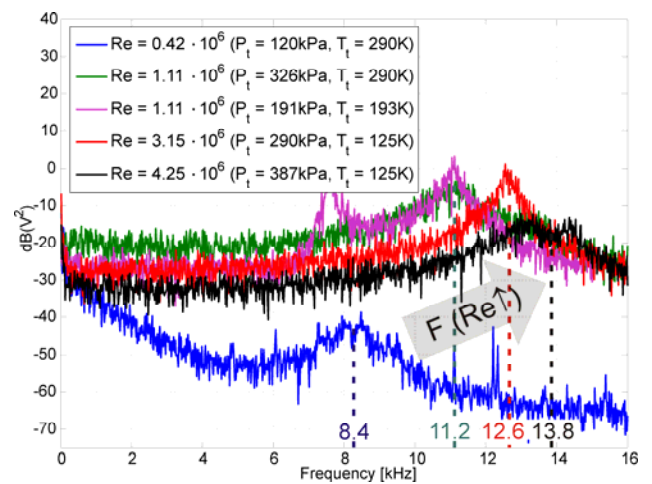


Fig.15: Power spectra of a selected surface hot-wire sensor ($x/c = 0.10$) at various Reynolds numbers, $\alpha_\infty = 3.0^\circ$ and $M_\infty = 0.2$

4. Assessment of deformation of model & model components

Performing systematic pure aeroelastic and Reynolds number investigations on a full aircraft model in ETW during the 2nd half of the nineties did prove even so called “rigid models” to be subject to deformation when tested in pressurised tunnels. Subsequently, ETW have developed techniques to assess the span wise distribution of wing twist and bending nowadays applied as a standard during each campaign. Starting with a Moiree-system and striving for an accuracy of 1mm in bend and 0.1 deg in twist ETW presently operates 2 independent Stereo Pattern Tracking systems (SPT) providing online data during testing. These systems rely on tracing the shift of markers attached to the components under consideration as shown in Fig. 16. While the leading system monitors the aeroelastic behaviour of the main wing the 2nd SPT is focussed on the flap (smaller markers).

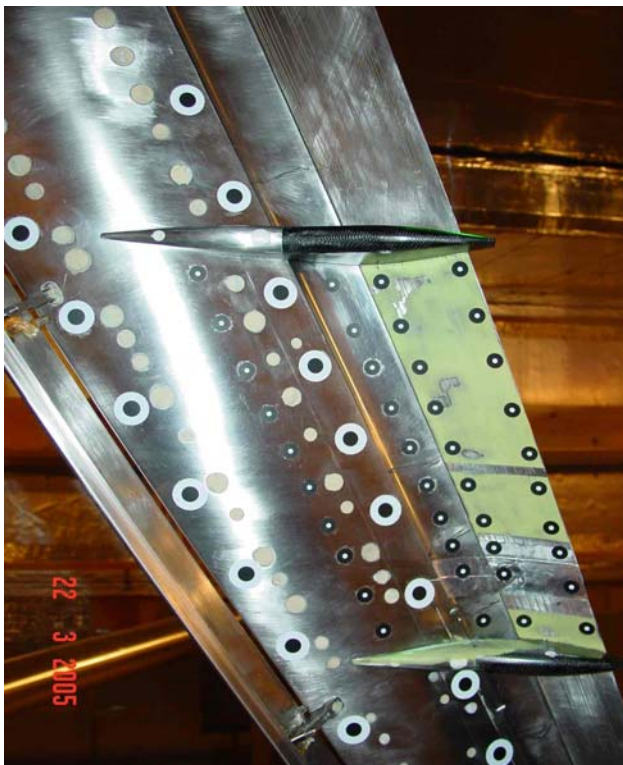


Fig.16: SPT markers for deformation assessment on main wing and flap of a high lift configuration

In a similar way the systems offer the capability to monitor the behaviour of the fin or the HTP.

More recently, customers expressed also interest in flap-gap monitoring. As the deformation assessment is based on the determination of the marker’s movement in space also the flap-gap is defined by the difference between the trailing edge of the main wing and leading edge of the flap. An elaborated sample is given in Fig. 16.

The rise in flap-gap height at a specific span-wise station is given as function of the model lift coefficient revealing a non-linear increase. In this first exercise an uncertainty of ± 0.5mm may be quoted but the assessed trend reveals a good repeatability. For more detailed analysis the individual flap attachments as well as the positioning of the individual markers have to be taken into account.

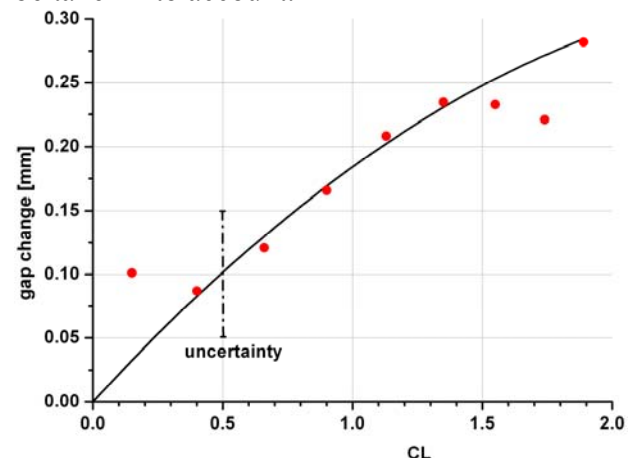


Fig.17: Assessment of flap –gap height as function of lift

5. Flow analysis by surveying

High operating cost of modern tunnels exclude the application of any point measurements of the flow field, so only 2d and 3d-techniques remain suitable. Here, the assessment of local velocity components is of primary interest.

5.1 Applying Doppler-Global Velocimetry

First successful trials to establish and operate a Doppler Global Velocimetry system in ETW have been reported in [9,10]. It could be demonstrated by using temperature conditioned housings for the optical components as well as image fibres that a wing tip vortex may be identified quantitatively, when generating seeding particles by an injection of water vapour mixed with gaseous nitrogen.

The drawback of this approach is its operating range limited to temperatures below the tunnel dew point, in practice about 200 K.

Driven by the request to provide validation data for CFD alternative seeding materials suitable for covering the complete test range of the facility have to be identified.

5.2 First Steps towards cryo-PIV

The Particle Image Velocimetry (PIV) is a well-developed non-intrusive measurement technique to determine unsteady as well as time averaged velocity vector fields inside a slice of the flow field [11]. For PIV measurements, the flow is seeded with small flow tracers. Using high energy pulse lasers, a thin light sheet illuminates the measurement plane in the flow. The light scattered by the particles inside the light sheet is recorded by specific cameras. Then, a digital correlation analysis is applied to successively recorded images to determine the particle shifts locally from which the flow velocity vectors can be calculated [12]. The measured vector fields can be further analyzed to determine characteristic flow parameters such as vorticity distributions, turbulent fluctuations or the circulation strengths of vortices for instance. Flow separations at rudders or flaps, for example, or the generation of vortices at interfaces and flow control devices can be visualized and their interaction with the flow on the wing can be investigated quantitatively. The possibility to apply PIV in facilities like the ETW is of particular interest since this would allow for investigations of flow phenomena under the same Mach and Reynolds numbers of real transport aircraft. However, the specific operating conditions at ETW as the cryogenic flow temperatures and the pressurized plenum surrounding the test section require further developments of the PIV technique. This is addressed within the nationally funded Cryo-PIV project of DLR and ETW.

The main problems and issues addressed in this project are:

- The generation of suitable tracer particles in ambient and cryogenic

flows.

- The optical access of a high energy laser light beam to the test section.
- Compensation of light deflections due to pressure and temperature changes.

Remotely controllable components like camera setups and mirrors may have to be placed inside the plenum. For applications of PIV at transonic speeds flow tracers in order of 1 μm are required to ensure that the particles follow the flow sufficiently. A moderate concentration and homogeneous distribution in the flow is necessary to get a good spatial resolution of the measured vector field. Specific flow seeding techniques are necessary for cryogenic wind tunnels. Fig. 18 shows the result of a Stereo-PIV measurement in a cryogenic low-speed wind tunnel (DNW-KKK) at a flow temperature of 150 K for which oil droplets are generated using DLR's droplet generators. In ETW however, oil may contaminate the insulation material or block the screens when freezing. Therefore, new substances and techniques are under development to generate tracers producing suitable signals for PIV and which can be easily removed from the wind tunnel circuit without leaving residua. Eventually, different stuff has to be used for different temperature ranges. Although the use of tiny ice particles revealed qualified the underlying physics are complicated so that tests are necessary to investigate the effects of ice particle formation, their growing and sublimation in dependency of the total pressure and temperature. Such tests are currently conducted within PETW and comprise different generation methods as well as alternative particle substances. The high flow rates of the ETW reached at transonic speeds require also a specific design of the seeding generator installation to be able to provide the required huge amount of particles of high quality with reproducible properties.

Another problem is laser beam deflection which occurs especially inside pressurised wind tunnels as observed in the transonic wind tunnel in Göttingen (DNW-TWG) [13]. Motorized mirrors and laser beam position detectors are necessary to be placed within the wind tunnel plenum to keep the light sheet in

place with respect to the model. The large plenum of 10m diameter and the limited optical access requires that the optics forming a thin light sheet must be placed within the plenum in front of a test section window. All optical components as well as the cameras must be placed within temperature controlled boxes. Since, these components are no longer accessible after tunnel closure all necessary adjustments have to be remotely controllable. Additionally, the operational costs of the ETW make it in particular essential that the whole measurement system and controlling units work robust to avoid off times. A demonstration test in the ETW is foreseen at the end of the Cryo-PIV project (2009), applying PIV to the flow of a realistic aircraft configuration

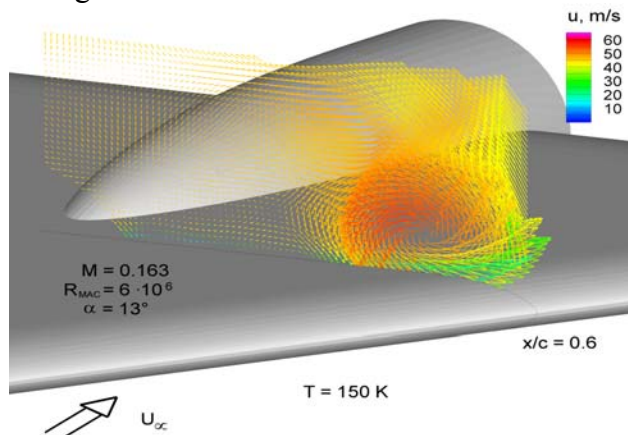


Fig 18: In-plane velocities (vectors) and out-of-plane velocities (vector color) above a delta wing obtained at T = 150 K.

6. Summary

The status of maturity and development on measurement techniques suitable for application in the pressurised cryogenic wind tunnel ETW is presented. Due to the thin boundary layers characterising high Reynolds number flow conditions the provision of an adequate surface finish is the primary issue. All techniques requiring particle seeding presently rely on the experimentally validated water vapour approach although alternative solutions are under investigation.

Further development work is progressing on all presented methods.

7. References

- [1] C. Tropea, J. Foss and A. Yarin [Ed.]: *Springer Handbook of Experimental Fluid Mechanics*, Chap. 7.4: “Transition Detection by Temperature-Sensitive Paint”, Springer, Heidelberg, 2007
- [2] Fey, U., Engler, R. H., Egami, Y., Iijima, Y., Asai, K., Jansen, U., and Quest, J. “Transition Detection by Temperature Sensitive Paint at Cryogenic Temperature in the European Transonic Wind Tunnel (ETW)”, *Proceedings of 20th International Congress on Instrumentation in Aerospace Simulation Facilities (ICIASF)*, Record, Göttingen, Germany, 2003, pp.77-88.
- [3] Iijima, Y., Egami, Y., Nishizawa, A., Asai, K., Fey, U., and Engler, R. H. “Optimization of Temperature-Sensitive Paint Formulation for Large-Scale Cryogenic Wind Tunnels”, *Proceedings of 20th International Congress on Instrumentation in Aerospace Simulation Facilities (ICIASF)*, Record, Göttingen, Germany, 2003, pp.70-77.
- [4] Y. Egami, U. Fey and J. Quest: “Development of New Two-Component TSP for Cryogenic Testing”, 45th *AIAA Aerospace Sciences Meeting and Exhibit*, Reno, NV, USA, Jan. 8-11, 2007, AIAA-2007-1062
- [5] Gaudet, L., Gell, T.G., Use of liquid crystals for qualitative and quantitative 2d studies of transition and skin friction, RAE TM Aero 2159, 1989.
- [6] Schulz, M., Quest, J., New techniques for operation in cryogenic wind tunnels, AIAA-2007-749.
- [7] Greff, E. In-flight measurement of static pressures and boundary-layer state with integrated sensors. *Journal of Aircraft*, Vol. 28, pp. 289–299, 1991.
- [8] Sturzebecher, D., Anders, S., Nitsche, W. The surface hot wire as a means of measuring mean and fluctuating wall shear stress, *Experiments in Fluids*, Vol. 31, pp. 294-301.
- [9] Willert, C., e.a. , Application of Doppler Global Velocimetry in Cryogenic Wind tunnels, *Experiments in Fluids*, Springer Verlag.
- [10] Willert, C., On the development of Doppler Global Velocimetry for cryogenic wind tunnels, 10th ICIAF, Goettingen, Germany, August 2003.
- [11] 2005 Kompenhans J, Raffel M, Dieterle L, Dewhurst T, Vollmers H, et al. Particle Image Velocimetry in Aerodynamics: Technology and Applications in Wind Tunnels. *Journal of Visualization*, Vol. 2, No 3/4, pp 229-244, 2000.
- [12] Raffel M, Willert CE, Wereley ST, Kompenhans J. Particle Image Velocimetry - A Practical Guide, 2nd Ed., Springer Berlin, ISBN 978-3-540-72307-3, 2007.
- [13] Schröder A, Agocs J, Frahnert H, Otter D, Mattner H, Kompenhans J, Konrath R. Application of stereo PIV to the VFE-2 65 delta wing configuration at sub- and transonic speeds, AIAA Paper 2006–3486, 2006.

Copyright Statement

The authors confirm that they, and/or their company or institution, hold copyright on all of the original material included in their paper. They also confirm they have obtained permission, from the copyright holder of any third party material included in their paper, to publish it as part of their paper. The authors grant full permission for the publication and distribution of their paper as part of the ICAS2008 proceedings or as individual off-prints from the proceedings.